NASA CONTRACTOR REPORT

NASA CR-4

NASA CR-401

A COMPUTER PROGRAM FOR CALCULATING THE CHARGE DISTRIBUTION ABOUT A SPACE VEHICLE

by Lee W. Parker

Prepared under Contract No. NAS 5-9088 *by*
MT. AUBURN RESEARCH ASSOCIATES, INC.
Cambridge, Mass.
for Goddard Space Flight Center

NATIONAL AERONAUTICS AND SPACE ADMINISTRATION • WASHINGTON, D. C. • MARCH 1966

NASA CR-401

A COMPUTER PROGRAM FOR CALCULATING THE CHARGE DISTRIBUTION ABOUT A SPACE VEHICLE

By Lee W. Parker

Prepared under Contract No. NAS 5-9088 by
MT. AUBURN RESEARCH ASSOCIATES, INC.
Cambridge, Mass.

for Goddard Space Flight Center

NATIONAL AERONAUTICS AND SPACE ADMINISTRATION

For sale by the Clearinghouse for Federal Scientific and Technical Information
Springfield, Virginia 22151 – Price $2.00

ABSTRACT

The distribution of charge about a space vehicle moving in the ionosphere (e.g., a satellite or probe) is given by the simultaneous solution of the Poisson and Boltzmann equations. One method for obtaining a self-consistent solution employs a computer code which takes into account the details of particle trajectories. A computer program is described in which the space in the vicinity of the object is represented by a discrete grid of points on which the potential and charge density distributions are defined. The advantage of such a purely numerical scheme is that conditions not amenable to analytic methods may be considered. For example, arbitrary velocities, body shapes and potentials, particle-surface interactions, magnetic fields, particle velocity distributions, and Mach numbers may be included. The program is straightforward and consists of two parts, one of which computes the densities on the grid when the potential is given. The other solves the Poisson problem on the grid when the densities are given. A self-consistent solution is sought by means of an iteration technique which may be started with a guessed potential distribution as initial input to the density calculation. The result of the density calculation becomes the input to a new Poisson problem which results in an improved guess for the potential distribution. The prescription for obtaining rapid convergence is largely a matter of art and is presently being investigated. The effects of variations in numbers of trajectories, trajectory step size, and grid dimensions, will be discussed, as well as the application of the method to a current satellite probe problem.

1. INTRODUCTION

The interaction of a charged object with a plasma results in the formation of a sheath which tends to shield the electrostatic field of the object from the plasma particles (e.g., a probe).

A kinetic-theoretical description of this effect is given by the simultaneous solution of the Boltzmann and Poisson equations resulting in self-consistent charged particle and electrostatic field distributions.

Approximate time-independent solutions for the collision-free satellite problem have been obtained by various investigators for the limiting case of high vehicle velocity (Mach number). It has been assumed, for example, that the ions are not affected by the electric field;[1, 2] that the ions have no random velocity;[3] or that the ions undergo very small deflections in the electric field.[4] Another interesting limiting case is the special one of a stationary planar, cylindrical, or spherical probe, where the high symmetry allows the problem to be described in terms of only one space variable.[5, 6, 7, 8] However, no analytic or numerical method has been developed for solving these problems under less restrictive assumptions. A purely numerical method would have the enormous advantage of being capable of including vehicle velocities, vehicle shapes and potentials, particle-surface interactions, magnetic fields, and particle velocity distributions in the ambient plasma, all of which may be arbitrarily specified. The numerical approach has the inherent disadvantage, however, of requiring unlimited computer speed and storage capacity in the absence of applied physical insight. It is the purpose of the present investigation to reduce the computer requirements by employing physical assumptions which do not vitiate the capacity of the computer program to handle complicated boundary conditions.

A computational procedure for determining mutually consistent charged particle and electrostatic potential distributions would be an iterative one requiring the performance of the two tasks:

A. Compute the charge density distribution, assuming the potential field is known. (The "Density" program.)

B. Compute the potential field, assuming the charge density distribution is known. (The "Poisson" program.)

The iteration procedure is begun with a guess, say for the potential field. First, task A is performed to compute the particle densities corresponding to the guessed field. Then these densities are used as inputs to the task B problem which results in a new potential field. This in turn becomes the input to a new task A problem. If the procedure converges, the potentials (or densities) of two successive cycles will eventually become equal, and will then be accepted as the solution.

The output of task A, the density calculation, is the heart of the problem, since methods are well known for solving task B, the Poisson problem.[9] The primary contribution of this paper has, therefore, to do with methods for computing particle densities and currents when the field is given.

The density of particles at a point $\vec{r}$ in space may be written as the triple integral

$$n(\vec{r}) = \iiint f(\vec{r}, \vec{v})\, d^3\vec{v} \qquad (1)$$

where $\vec{r}$ and $\vec{v}$ are, respectively, the local position and velocity vectors, and the integrand f is the function which satisfies the Boltzmann equation. In the collision-free case, the function f is a constant along each trajectory defined by the pair of vectors $\vec{r}$, $\vec{v}$. At the "other end" of each trajectory the function f is assumed known, for example, at infinity or on the surface of the vehicle. If the velocity distribution at infinity is a Maxwellian characterized by a temperature (T) and an ambient part density (n_o), then in a coordinate system in which the vehicle is stationary the function f is given, for those trajectories

which originate at infinity, by:

$$f = f_\infty \equiv \frac{n_o}{\pi^{3/2}} e^{-v_\infty^2 - v_s^2 + 2v_\infty v_s \cos\alpha} \qquad (2)$$

with

$$v_\infty^2 = v^2 + \phi \qquad (3)$$

where v and v_∞ are the magnitudes of the local velocity and the velocity at infinity, respectively, in units of $(2kT/m)^{\frac{1}{2}}$ where m is the particle mass, ϕ is potential energy of the particle at $\vec{r}$ in units of kT, v_s is the magnitude of the vehicle velocity in units of $(2kT/m)^{\frac{1}{2}}$, i.e., the Mach number, and α is the angle between the vectors $\vec{v}_\infty$ and $\vec{v}_s$.

For those trajectories which originate at the surface of the vehicle the appropriate distribution function is to be used for f in Eq. (1). If there is no surface emission, f is set to zero. For other particle-surface interactions, an appropriate value of f may be assigned. If the trajectory corresponds to a trapped particle it will be considered unpopulated (f = 0) in the absence of collisions.

Thus, the problem of the density calculation is that of determining the demarcation between those trajectories which originate at infinity and those which do not (e.g., trapped or emitted particles). In the theory of the spherical and cylindrical probe by Mott-Smith and Langmuir[5] it is in effect assumed that every trajectory of positive total energy connects with infinity. However, the revised versions of spherical and cylindrical probe theory by Bernstein and Rabinowitz[6] and Hall[7] take account of trajectories which, though energetically capable of doing so, do <u>not</u> connect with infinity. As a result, there may be a portion of the velocity space in which the integrand in Eq. (1) is zero, even for trajectories having positive total energy. Since the boundary of the forbidden portion of velocity space is an unknown function of the potential

distribution in position space, the integral in Eq. (1) is difficult to evaluate analytically. Bernstein and Rabinowitz[6] evaluated it for an isotropic monoenergetic particle velocity distribution at infinity, but numerical methods are required for the isotropic Maxwellian.[7, 8] In the stationary spherical or cylindrical probe problem, the symmetry makes possible a great simplification which depends in a fundamental way on the constancy of angular momentum. The case of a moving object presents much greater analytic difficulties.

In Section 2, the method of evaluating the density integral Eq. (1) by summing over trajectories is described. In Section 3, the OGO satellite probe geometry is defined and the approximate analytic Laplace solution is presented. In Section 4, the method of calculating probe currents and the grid representation for a potential field are described. The trajectory calculations are discussed in Section 5. In Section 6, the current vs voltage calculations are presented, on the assumption of no space charge effects (Laplace field). The Poisson problem and density calculations are discussed in Section 7. The iteration procedure and results are given in Section 8.

2. THE SUM OVER TRAJECTORIES

In the general problem, the detailed trajectories of the particles must be calculated. A numerical evaluation of the integral in Eq. (1) may be carried out by replacing it approximately by a discrete triple quadrature of the form

$$n(\vec{r}) = \sum_{k}^{N_1} \sum_{\ell}^{N_2} \sum_{n}^{N_3} A(k, \ell, n)\, f_{\infty}(k, \ell, n) \qquad (4)$$

where the indices k-ℓ-n refer to the velocity vector $\vec{v}(k, \ell, n)$ which characterizes the $(k$-ℓ-$n)$th trajectory. The function f_{∞} is obtained from Eqs. (2) and (3) by tracing the $(k$-ℓ-$n)$th trajectory backwards in time to its source. If the source is at infinity, $v(k, \ell, n)$ is used in Eq. (3), and the computed limiting value of α in Eq. (2).

The coefficient $A(k, \ell, n)$ is a coefficient which depends on the quadrature scheme used (e.g., Gaussian), and which vanishes if the trajectory corresponds to a trapped particle or if it originates on a non-emitting surface. The accuracy of the trajectory sum in Eq. (4) may be increased by increasing the product $N_1N_2N_3$, i.e., the number of trajectories.

In general, the potential field must be given as a function defined on a grid of space points in the vicinity of the vehicle. A magnetic field may also be defined on the same grid.

The particle is considered as having reached "infinity" when it passes through the outer boundary of the grid.

The other half of the self-consistent calculation, i.e., the Poisson problem, may be solved on the same grid of space points through the replacement of the Poisson equation by a set of simultaneous difference equations for the discrete values of the potential. These are to be solved subject to the conditions that the potential vanish at infinity and that it be equal to the vehicle potential at the vehicle surface.

3. THE OGO PROBE PROBLEM

The ideas of the preceding discussion are being applied to the problem of computing the space charge and potential distributions in the vicinity of a planar ion and electron trap experiment[10] on the Orbiting Geophysical Observatory satellite. The objective of the experiment is to infer the particle velocity distribution in the ambient ionosphere plasma from the velocity distribution measured at the aperture of the probe. The procedure might be to compute the aperture distributions which would be associated with various hypothetical ambient distributions and to compare these with the observed one.

The probe geometry is shown in Fig. 1, which is not drawn to scale. The probe consists of a circular opening in the skin of the satellite below which is a plate maintained at a potential V_o with respect to the satellite. The separation between the plate and the satellite skin is about 1/35 of the radius of the hole. Part of the plate consists of a grid, the collecting aperture, whose radius is $\frac{1}{2}$ that of the opening. Below this grid is a current-collecting electrode (not shown in Fig. 1) whose voltage is variable with respect to the grid. The theoretical problem is that of computing the particle velocity distribution at the grid plane when the grid voltage V_o and the velocity distribution at infinity are given.

Since the depth of the grid plane below the level of the outer surface of the satellite skin is less than 1/13 the hole radius, the probe geometry may be approximated by an infinite plate surrounding a circular disc which is maintained at a different potential, schematically shown in Fig. 2. In the following, the disc will be referred to as the "probe".

The plate is considered in this approximation to extend to infinity since the dimensions of the satellite are large compared with the probe radius. The satellite is also large compared with the Debye length. The question of the effect of the sheath of the satellite on the probe characteristics is not considered here. It is assumed that

the effect is negligible if the probe potential is large compared with kT while the satellite potential is of the order of kT, where T is the temperature of the ambient plasma.

Under the stated assumptions, the unshielded Laplace field in the neighborhood of the probe can be expressed analytically in the form

$$V(r, z) = V_o \int_o^\infty e^{-\frac{z}{a} x} J_1(x) J_o(\frac{r}{a} x) dx \qquad (5)$$

where a is the radius of the probe, z and r are cylindrical coordinates for the problem, which is restricted to be rotationally symmetric about the z-axis, J_1 and J_o are Bessel functions of order one and zero, respectively, and V_o is the potential of the probe (i.e., the circular disc) with respect to the infinite plane. The Laplace solution for $V_o = 1.0$ is tabulated in Table I and expressed in terms of contours in Fig. 2. The potential distribution for V_o other than 1.0 is obtained from these by multiplying by V_o.

The asymptotic form for the potential is given by

$$V(r, z) \sim \frac{V_o a^2}{2} \frac{z}{(r^2 + z^2)^{3/2}} \qquad (6)$$

which is the potential of a dipole of moment $\frac{1}{2} V_o a^2$.

4. CURRENT-VOLTAGE CHARACTERISTICS

Before proceeding to the space charge calculations, we will discuss the application of the numerical method to the calculation of the current-voltage characteristics of the Laplace field given by Eq. (5). The same ideas will be applied to the Poisson problem later. The potential field is described by a discrete grid in r - z space such as that shown in Fig. 3. In Fig. 3, the r-domain is divided in 12 equal intervals, with r going from 0(i = 1) to r_m(i = 13). The z-domain is divided in 12 equal intervals also, with z going from 0(j = 1) to z_m(j = 13). The column i = 1 (r = 0) represents the axis of the system, which is presently rotationally symmetric. The row j = 1 (z = 0) represents the plane of the probe, on which the point i = 1, j = 1 represents the center of the circular probe area, i.e., the center of the grid in Fig. 1. The point r = a, that is, the radius of the probe, is chosen to be some point on the first row, defining the r-scale. In Fig. 3, this point is i = 5, j = 1.

The outer boundary of the grid is defined by r_m and z_m, at which the particles are assumed to have a Maxwellian distribution, shifted by the plasma velocity. The z-axis of the problem is defined by the normal to the probe, which is assumed parallel to the plasma velocity vector. The device of using an outer grid boundary to represent "infinity" is only valid if the dimensions of the boundary are sufficiently large that the resulting solution is independent of their value. The Laplace field may be taken from Table I if the scales are appropriately chosen. If the point i = 5 in the first row represents the probe radius a = 3.33 cm (see Fig. 1), then r_m = 3a = 9.99 cm and Δr = .8325 cm. If z_m is chosen to be 1.5a = 4.995 cm, then Δz = .41625 cm. The quantities Δr and Δz may be designated as "grid spacings". In Table I, Δr and Δz are both equal to a/4 (ignoring the 0.1 row). The potentials obtained from Table I are to be multiplied by the appropriate scale factor such that the potentials on the first 4 points in the first row in Fig. 3 have the probe potential. The 5th point is assigned ½ of

this value. In Fig. 3, the probe potential is -5.1 volts, corresponding to an ion potential energy -45.54 kT.

The current density at a point $\vec{r}$ on the probe is obtained by evaluating the first moment of the distribution, i.e., the integral

$$j(\vec{r}) = \iiint f(\vec{r}, \vec{v})\ v_z d^3\vec{v} \qquad (7)$$

where j is the current density normal to the probe and v_z is the z-component of velocity. This triple integral is similar to Eq. (1) and may be treated in the same manner using a triple quadrature in a form similar to Eq. (4), where the trajectories are treated exactly as in the discussion of Eq. (4).

5. TRAJECTORY CALCULATIONS

For the trajectory calculations, the following units have been adopted. The unit of energy is kT. The unit of velocity is $(2kT/m)^{\frac{1}{2}}$. The unit of length is the Debye length, λ_D, which is taken to be exactly one centimeter, corresponding to an altitude of about 200 km, where the temperature (T) is assumed to be $1300^{\circ}K$ and the electron density (n_o) is assumed to be 6×10^4 particles/cm^3. The symbol ϕ is used for the dimensionless potential energy, which is negative for attracted particles and positive for repelled particles. Thus, if the probe potential is -5.1 volts, the dimensionless probe potential is $\phi_o = +45.54$ for electrons and -45.54 for singly-charged ions. The only relevant mass-dependent quantity in the problem is the Mach number.

A trajectory may be described by the solution of the simultaneous dynamical equations in cartesian form:

$$\ddot{x} = -\frac{1}{2}\frac{x}{r}\frac{\partial\phi}{\partial r}$$

$$\ddot{y} = -\frac{1}{2}\frac{y}{r}\frac{\partial\phi}{\partial r} \qquad (8)$$

$$\ddot{z} = -\frac{1}{2}\frac{\partial\phi}{\partial z}$$

The unit of time, $\lambda_D(m/2kT)^{\frac{1}{2}}$, is irrelevant since the intervals of time, Δt, must only be chosen short enough to obtain an arbitrarily accurate description of the particle path in space. Empirically, the required accuracy is determined by making test runs with successively smaller time step sizes until the sequence of densities or currents converges. The gradients $\partial\phi/\partial r$ and $\partial\phi/\partial z$ in Eq. (8) are obtained by interpolation within the potential grid. The trajectory is followed backwards in time, where the initial values of x, y, z are given by the components of $\vec{r}$ and the initial values of $\dot{x}$, $\dot{y}$, $\dot{z}$ by the components of the velocity vector $\vec{v}(k, \ell, n)$ which characterizes the $(k\text{-}\ell\text{-}n)$th trajectory in the triple sum. The trajectory is followed until it either strikes the (non-emitting)

plate or passes out of the boundary. A trajectory is considered as trapped if it spends too much time meandering within the grid. Thus, if the total arc length exceeds a reasonable value, the value of f is set to zero.

There are several methods[11] for integrating Eq. (8), such as a predictor-corrector, a Runge-Kutta method, or a Taylor series. The Taylor series was chosen for simplicity and truncated beyond the second derivative terms. Use of a higher-order method such as a predictor-corrector did not appear justified when used in coarse potential grids in the preliminary phases of the work. However, the accuracy of the computed densities and currents was found to depend strongly on the accuracy of the trajectories.

The number of trajectories used for a density point is determined by the orders of the quadrature scheme adopted for Eq. (4). The scheme adopted here has been the Gaussian triple quadrature. In some of the calculations, the orders 64, 32, and 8 were used for the velocity components, namely, the speed (index k), the polar angle (index ℓ), and the azimuthal angle (index n), respectively. The number of trajectories was therefore 16384 per density point. This large number gave accuracies ranging from 1 part in 10^6 to 1 part in 10^4 for zero potential for Mach numbers up to 7. However, the computing time was very great, i.e., several minutes per point. In the calculations for the Laplace field at zero Mach number, the orders 16, 8, and 8 (or 1024 trajectories) were found to give accuracies varying between 1% and 30%, depending on the potential field and the position of the density point.

6. CURRENT VS VOLTAGE FOR THE LAPLACE FIELD

Tables II, III and IV represent the Laplace field for a probe potential of -5.1 volts. In Tables II and III, the same space is represented by a 13 x 13 grid and a 4 x 4 grid, respectively. For these tables, the radius and height of the outer boundary of the grid are at $r_m = 3a$ and $z_m = 1.5a$, respectively. In Table IV, a 13 x 13 grid represents a space of the same radial dimension, $r_m = 3a$, but of height $z_m = 3a$. For the grids in Tables II, III, and IV, the currents are 36, 34, and 35, respectively. They are expressed in units of the zero-potential current, namely:

$$J_o \equiv An_o(kT/2\pi m)^{\frac{1}{2}} \left[e^{-v_s^2} + \sqrt{\pi}\, v_s\, (1 + \text{erf}\, v_s)\right] \qquad (9)$$

where A is the current-collecting area and v_s is the Mach number.

The values 36, 34,and 35 for the currents are equal to within the accuracy of the calculation. They were obtained by using a small trajectory step size, about 0.2 per step in units of λ_D. When the step size was 0.4 and 0.8, the values of the 3 currents differed by as much as 100% from one another. From these calculations it may be concluded that the effects on the Laplace field current of increasing r_m or z_m, or the number of grid points, is small compared with the effect of the step size, i.e., the accuracy of the trajectory calculations.

Current-voltage characteristics are shown in Fig. 4 for the Laplace fields of Tables II, III, and IV. These lie close to one another and are represented approximately by straight lines which have the equation $J/J_o = 1 - .75\phi$ This may be compared with the Langmuir formula $1 - \phi$ for a sphere. The linear term may be tentatively associated with geometrical effects which may diminish it, such as intersections with the satellite. The constant term, on the other hand,probably depends only on the energy distribution at infinity.

A current-vs-Mach number curve is shown in Fig. 5 for a probe potential of -5.1 volts. The current decreases from a large value

asymptotically to unity. The currents for small Mach numbers are not accurate, since the step size was large, corresponding to an arc length of about .8 per step. The grid was a 7 x 7, with $r_m = z_m = 1.5a$.

Some distributions in energy, dJ/dE, of the particle currents arriving at the aperture were calculated for probe potentials of zero and -5.1 volts. The energies are associated with the z-components of particle velocity. The distributions are given in Table V for three cases:

(a) potential zero and Mach 7

(b) potential -5.1 volts and Mach zero

(c) potential -5.1 volts and Mach 7

The currents for case (a) agree exactly with the theoretical expression (see Table V) for all values of the energy. The currents for case (b) satisfy the exact exponential law for energies greater than 5.1 volts, but are less than unity for energies less than 5.1 volts. The deficiency is consistent with the reduced slope (.75) of the current-voltage curve and is probably due to trajectory intersections with the satellite. The results of case (b) suggest that the energy distribution represents the distribution at infinity quite accurately, i.e., an exponential, for particle energies greater than the probe potential. For energies less than the probe potential, the distribution appears to be affected by the geometry of the probe. In case (c), the maximum of dJ/dE lies beyond 8.4 volts.

7. THE POISSON PROBLEM

For the solution of the Poisson equation, a difference equation was used to approximate the Laplacian operator in cylindrical coordinates. The boundary condition was unusual in that an asymptotic analytic form was assumed to represent the potential outside the boundary. The coefficient was an unknown quantity, to be determined such that the potential and its partial derivatives were continuous. Since there were three equations for each boundary point, the system was over-determined and a least-squares matrix reduction was employed. The idea of using an asymptotic form is based on the success with which Laframboise[8] obtained numerical self-consistent solutions to the spherical probe problem with the grid boundary close to the sphere surface. Laframboise adopted the r^{-2} asymptotic law derived by Bernstein and Rabinowitz[6] for the mono-energetic distribution. However, in the absence of an asymptotic theory for the general problem, it is not clear how to choose the form for such a function.

In the present work, solutions of the Laplace equation were found using various asymptotic forms for the potential. The dipole form, Eq. (6), was tried, as well as several other forms and combinations thereof. The Laplace solution depended rather strongly on the choice of the form. The dipole term gave excellent agreement with the exact values in Table I. Attempts were made to solve the non-linear equations to determine the exponent in the asymptotic power law, but this was not pursued far enough to determine the effectiveness of the method. While perhaps promising, it would probably require excessive computer time. The dipole law was adopted provisionally for the space charge calculations.

Attempts were also made in the density calculations to obtain some idea of the effects of the asymptotic force law beyond the boundary. A first-order velocity correction based on an impulse approximation was applied to the trajectories at the grid boundary. This produced at most a change of a few percent, even for Mach 7.

The densities at the grid points of the Laplace field defined by

Table II are shown in Table VI. These were obtained from Eq. (4) by essentially the same method as was used for computing currents. The Mach number was zero. The number of trajectories used was 1024, and the trajectory step size used varied with the position of the grid point. For points on the probe surface, for example, the arc length per step was about .2, while for points on the boundary it was 3.2. This scheme sufficed to keep the estimated overall accuracy within 10%. At a few places, the error in density was 30%. The 169 values of the ion density (attracted particles) were obtained in about 10 minutes. The electron densities (repelled particles) were obtained in about 3.5 minutes by reversing the sign of the potential field.

8. SELF-CONSISTENT SOLUTION

In the iteration scheme, the initial guessed potential field was designated the "zero-order" potential, and the densities resulting therefrom the "zero-order" densities. Thus, the Laplace field in Table II was chosen as the zero-order potential, and the densities in Table VI were the zero-order densities. These densities were used in the Poisson problem to obtain a "first-order" potential, which resulted in "first-order" densities. The iteration converged in the sense that the 6th-order potential was reproduceable to 2 significant figures, with minor exceptions. The Poisson potential for a probe potential of -5.1 volts is shown in Table VII and the associated self-consistent densities in Table VIII. A definite sheath region is evident from the electron distribution.

More rapid convergence was obtained by coupling the densities of successive iterations. That is, the newest set of densities was averaged with the previous input set to obtain the next input set. The zero-order densities were averaged with zero, i.e., divided by 2, to obtain the input to the first-order potential. This procedure reduced the number of iterations to 3, instead of 6, to produce the self-consistent potential shown in Table VII. The sequence of iterates was oscillating rather than monotonic.

The fact that convergence was achieved rather easily is probably connected with the fact that the solution grid (Table VII) still lies well within the sheath region; that is, some of the potentials along the upper boundary of the grid, where $z_m = 1.5a$, are considerably larger than kT. Attempts are being made to obtain convergence for grids for which $z_m = 3a$ and $z_m = 4a$. These appear to have more difficulty in converging, tending to oscillate much longer. This may be connected with the fact that the upper boundaries are outside the sheath, i.e., in the region where the potential is less than kT. Experimentation is in progress with very small grids, i.e., 3 x 3, 4 x 4, etc., to determine the numerical properties of the procedure. For example, the iterations

diverged in the absence of coupling for $z_m = 3a$ and $z_m = 4a$.

The probe current for the Poisson (self-consistent) field was 24, as compared with the zero-order value 36, at a probe potential of -5.1 volts. This point is indicated in Fig. 4, showing that a considerable reduction in current can be expected.

9. CONCLUSIONS

A numerical method and its application to the OGO probe experiment has been described. A current-voltage characteristic has been obtained for the Laplace field at Mach zero, and a self-consistent solution at one value of the probe potential. Rather coarse grids were found to describe the field well. However, it was found that the trajectory step sizes needed to be small compared with the grid spacing. The results obtained with an arbitrarily chosen form for the asymptotic potential (dipole potential) were found useful. An iteration procedure in which successive density iterates were coupled was found to converge more rapidly than when the iterates were uncoupled.

TABLE I

TABLE OF THE INTEGRAL $\int_0^\infty e^{-\frac{z}{a}x} J_1(x) J_o(\frac{r}{a}x)dx$

r/a =	.0	.25	.50	.75	1.00	1.25	1.50
z/a = 5.0	.1940(-1)	.1933(-1)	.1913(-1)	.1880(-1)	.1836(-1)	.1781(-1)	.1718(-1)
4.75	.2143(-1)	.2135(-1)	.2111(-1)	.2071(-1)	.2017(-1)	.1952(-1)	.1876(-1)
4.50	.2380(-1)	.2370(-1)	.2340(-1)	.2291(-1)	.2226(-1)	.2146(-1)	.2055(-1)
4.25	.2657(-1)	.2644(-1)	.2607(-1)	.2548(-1)	.2467(-1)	.2370(-1)	.2259(-1)
4.00	.2984(-1)	.2969(-1)	.2923(-1)	.2848(-1)	.2748(-1)	.2628(-1)	.2492(-1)
3.75	.3375(-1)	.3356(-1)	.3297(-1)	.3203(-1)	.3078(-1)	.2928(-1)	.2760(-1)
3.50	.3847(-1)	.3821(-1)	.3746(-1)	.3626(-1)	.3467(-1)	.3279(-1)	.3069(-1)
3.25	.4421(-1)	.4388(-1)	.4290(-1)	.4135(-1)	.3931(-1)	.3691(-1)	.3427(-1)
3.00	.5131(-1)	.5087(-1)	.4958(-1)	.4753(-1)	.4487(-1)	.4177(-1)	.3841(-1)
2.75	.6020(-1)	.5960(-1)	.5787(-1)	.5513(-1)	.5161(-1)	.4756(-1)	.4323(-1)
2.50	.7152(-1)	.7070(-1)	.6831(-1)	.6459(-1)	.5985(-1)	.5447(-1)	.4882(-1)
2.25	.8618(-1)	.8503(-1)	.8169(-1)	.7651(-1)	.7001(-1)	.6276(-1)	.5530(-1)
2.00	.1056	.1039	.9913(-1)	.9178(-1)	.8268(-1)	.7274(-1)	.6277(-1)
1.75	.1318	.1293	.1223	.1116	.9864(-1)	.8474(-1)	.7122(-1)
1.50	.1679	.1643	.1538	.1380	.1189	.9908(-1)	.8051(-1)
1.25	.2191	.2136	.1977	.1736	.1450	.1160	.9008(-1)
1.00	.2929	.2846	.2606	.2233	.1787	.1350	.9853(-1)
0.75	.4000	.3884	.3532	.2951	.2228	.1542	.1026
0.50	.5528	.5390	.4937	.4068	.2815	.1659	.9500(-1)
0.25	.7574	.7469	.7079	.6062	.3625	.1409	.6297(-1)
0.10	.9005	.8956	.8768	.8158	.4303	.7375(-1)	.2788(-1)
0.00	1.0000	1.0000	1.0000	1.0000	.5000	0.0	0.0

TABLE I Cont'd

TABLE OF THE INTEGRAL $\int_0^\infty e^{-\frac{z}{a}x} J_1(x)\, J_0(\frac{r}{a}x)\,dx$

r/a =	1.75	2.00	2.25	2.50	2.75	3.00	3.25
z/a = 5.0	.1648(-1)	.1572(-1)	.1493(-1)	.1412(-1)	.1331(-1)	.1250(-1)	.1171(-1)
4.75	.1792(-1)	.1703(-1)	.1610(-1)	.1516(-1)	.1421(-1)	.1328(-1)	.1238(-1)
4.50	.1955(-1)	.1849(-1)	.1739(-1)	.1629(-1)	.1519(-1)	.1412(-1)	.1309(-1)
4.25	.2138(-1)	.2011(-1)	.1881(-1)	.1751(-1)	.1624(-1)	.1501(-1)	.1383(-1)
4.00	.2346(-1)	.2193(-1)	.2038(-1)	.1885(-1)	.1736(-1)	.1593(-1)	.1459(-1)
3.75	.2581(-1)	.2396(-1)	.2210(-1)	.2029(-1)	.1854(-1)	.1690(-1)	.1536(-1)
3.50	.2848(-1)	.2622(-1)	.2399(-1)	.2183(-1)	.1979(-1)	.1788(-1)	.1613(-1)
3.25	.3151(-1)	.2874(-1)	.2604(-1)	.2347(-1)	.2107(-1)	.1887(-1)	.1687(-1)
3.00	.3495(-1)	.3153(-1)	.2824(-1)	.2518(-1)	.2236(-1)	.1982(-1)	.1755(-1)
2.75	.3884(-1)	.3459(-1)	.3059(-1)	.2692(-1)	.2363(-1)	.2070(-1)	.1814(-1)
2.50	.4322(-1)	.3790(-1)	.3302(-1)	.2864(-1)	.2480(-1)	.2146(-1)	.1858(-1)
2.25	.4809(-1)	.4141(-1)	.3545(-1)	.3024(-1)	.2578(-1)	.2200(-1)	.1881(-1)
2.00	.5339(-1)	.4499(-1)	.3772(-1)	.3157(-1)	.2645(-1)	.2223(-1)	.1875(-1)
1.75	.5896(-1)	.4840(-1)	.3960(-1)	.3243(-1)	.2665(-1)	.2202(-1)	.1831(-1)
1.50	.6441(-1)	.5120(-1)	.4071(-1)	.3252(-1)	.2617(-1)	.2124(-1)	.1741(-1)
1.25	.6898(-1)	.5271(-1)	.4053(-1)	.3149(-1)	.2478(-1)	.1975(-1)	.1594(-1)
1.00	.7122(-1)	.5185(-1)	.3837(-1)	.2893(-1)	.2224(-1)	.1741(-1)	.1385(-1)
0.75	.6861(-1)	.4714(-1)	.3345(-1)	.2447(-1)	.1840(-1)	.1416(-1)	.1113(-1)
0.50	.5741(-1)	.3699(-1)	.2519(-1)	.1793(-1)	.1322(-1)	.1004(-1)	.7808(-2)
0.25	.3399(-1)	.2070(-1)	.1365(-1)	.9526(-2)	.6936(-2)	.5221(-2)	.4032(-2)
0.10	.1436(-1)	.8569(-2)	.5590(-2)	.3877(-2)	.2815(-2)	.2116(-2)	.1630(-2)
0.00	0.0	0.0	0.0	0.0	0.0	0.0	0.0

TABLE I Cont'd

TABLE OF THE INTEGRAL $\int_0^\infty e^{-\frac{z}{a}x} J_1(x) J_0(\frac{r}{a}x)dx$

r/a =	3.50	3.75	4.00	4.25	4.50	4.75	5.00
z/a = 5.0	.1094(-1)	.1020(-1)	.9502(-2)	.8839(-2)	.8215(-2)	.7630(-2)	.7085(-2)
4.75	.1152(-1)	.1069(-1)	.9910(-2)	.9177(-2)	.8492(-2)	.7856(-2)	.7266(-2)
4.50	.1211(-1)	.1119(-1)	.1032(-1)	.9509(-2)	.8759(-2)	.8067(-2)	.7430(-2)
4.25	.1272(-1)	.1168(-1)	.1072(-1)	.9827(-2)	.9008(-2)	.8257(-2)	.7572(-2)
4.00	.1334(-1)	.1217(-1)	.1110(-1)	.1012(-1)	.9231(-2)	.8421(-2)	.7686(-2)
3.75	.1394(-1)	.1264(-1)	.1146(-1)	.1039(-1)	.9420(-2)	.8548(-2)	.7765(-2)
3.50	.1453(-1)	.1308(-1)	.1178(-1)	.1061(-1)	.9563(-2)	.8631(-2)	.7801(-2)
3.25	.1507(-1)	.1346(-1)	.1203(-1)	.1077(-1)	.9647(-2)	.8659(-2)	.7786(-2)
3.00	.1554(-1)	.1377(-1)	.1221(-1)	.1085(-1)	.9660(-2)	.8619(-2)	.7709(-2)
2.75	.1590(-1)	.1396(-1)	.1229(-1)	.1084(-1)	.9584(-2)	.8500(-2)	.7562(-2)
2.50	.1612(-1)	.1402(-1)	.1223(-1)	.1071(-1)	.9404(-2)	.8290(-2)	.7334(-2)
2.25	.1614(-1)	.1390(-1)	.1202(-1)	.1044(-1)	.9103(-2)	.7976(-2)	.7018(-2)
2.00	.1590(-1)	.1355(-1)	.1161(-1)	.1000(-1)	.8667(-2)	.7547(-2)	.6606(-2)
1.75	.1534(-1)	.1293(-1)	.1098(-1)	.9391(-2)	.8080(-2)	.6996(-2)	.6092(-2)
1.50	.1440(-1)	.1201(-1)	.1011(-1)	.8581(-2)	.7336(-2)	.6317(-2)	.5474(-2)
1.25	.1302(-1)	.1076(-1)	.8981(-2)	.7568(-2)	.6432(-2)	.5510(-2)	.4755(-2)
1.00	.1119(-1)	.9159(-2)	.7588(-2)	.6354(-2)	.5372(-2)	.4582(-2)	.3940(-2)
0.75	.8897(-2)	.7225(-2)	.5948(-2)	.4955(-2)	.4171(-2)	.3546(-2)	.3039(-2)
0.50	.6195(-2)	.5001(-2)	.4097(-2)	.3401(-2)	.2854(-2)	.2420(-2)	.2070(-2)
0.25	.3183(-2)	.2560(-2)	.2093(-2)	.1734(-2)	.1452(-2)	.1231(-2)	.1052(-2)
0.10	.1284(-2)	.1032(-2)	.8464(-3)	.7025(-3)	.5880(-3)	.4992(-3)	.4277(-3)
0.00	0.0	0.0	0.0	0.0	0.0	0.0	0.0

TABLE II

Laplace Potential For 13 x 13 Grid $r_m = 3a$, $z_m = 1.5a$

Probe Potential = -5.1 volts

(All values are negative for ions, positive for electrons)

		1	2	3	4	5	6	7	8	9	10	11	12	13
(1.5a)	13	7.3	7.1	6.5	5.5	4.5	3.6	2.8	2.1	1.6	1.3	1.0	.79	.66
	12	8.4	8.1	7.4	6.3	5.1	4.0	3.0	2.3	1.7	1.3	1.0	.78	.64
	11	9.6	9.3	8.5	7.2	5.8	4.5	3.3	2.4	1.8	1.3	.99	.76	.61
	10	11	11	9.8	8.3	6.6	5.0	3.6	2.5	1.8	1.3	.96	.73	.58
	9	13	13	11	9.6	7.5	5.5	3.8	2.6	1.8	1.3	.93	.69	.53
	8	15	15	13	11	8.5	6.0	4.0	2.7	1.8	1.2	.87	.64	.49
	7	18	17	16	13	9.7	6.5	4.2	2.7	1.7	1.2	.80	.58	.43
	6	21	20	19	15	11	7.0	4.2	2.6	1.6	1.1	.71	.50	.37
	5	25	24	22	18	13	7.2	4.1	2.4	1.4	.91	.60	.42	.31
	4	29	29	27	22	14	7.2	3.6	2.0	1.2	.72	.47	.32	.24
	3	34	34	32	27	17	6.5	2.9	1.5	.83	.50	.33	.22	.16
	2	40	39	38	35	19	4.5	1.6	.78	.43	.26	.17	.11	.08
	1	46	46	46	46	23	0	0	0	0	0	0	0	0

Current = 36 (3a)

TABLE III

Laplace Potential For 4 x 4 Grid $r_m = 3a$, $z_m = 1.5a$

Probe Potential = -5.1 volts

(All values are negative for ions, positive for electrons)

		1	2	3	4
(1.5a)	4	7.3	4.5	1.6	.66
	3	13	7.5	1.8	.53
	2	25	13	1.4	.31
	1	46	23	0	0
		Current = 34			(3a)

TABLE IV

Laplace Potential For 13 x 13 Grid $r_m = 3a$, $z_m = 3a$

Probe Potential = -5.1 volts

(All values are negative for ions, positive for electrons)

		1	2	3	4	5	6	7	8	9	10	11	12	13
(3a)	13	2.3	2.3	2.3	2.2	2.0	1.9	1.8	1.6	1.4	1.3	1.2	1.0	.90
	12	2.7	2.7	2.6	2.5	2.4	2.2	2.0	1.8	1.6	1.4	1.2	1.1	.94
	11	3.3	3.2	3.1	2.9	2.7	2.5	2.2	2.0	1.7	1.5	1.3	1.1	.98
	10	3.9	3.9	3.7	3.5	3.2	2.9	2.5	2.2	1.9	1.6	1.4	1.2	1.0
	9	4.8	4.7	4.5	4.2	3.8	3.3	2.9	2.4	2.1	1.7	1.4	1.2	1.0
	8	6.0	5.9	5.6	5.1	4.5	3.9	3.2	2.7	2.2	1.8	1.5	1.2	1.0
	7	7.7	7.5	7.0	6.3	5.4	4.5	3.7	2.9	2.3	1.9	1.5	1.2	.97
	6	10	9.7	9.0	7.9	6.6	5.3	4.1	3.1	2.4	1.9	1.4	1.1	.90
	5	13	13	12	10	8.1	6.2	4.5	3.2	2.4	1.8	1.3	1.0	.79
	4	18	18	16	13	10	7.0	4.7	3.1	2.2	1.5	1.1	.84	.65
	3	25	25	23	19	13	7.6	4.3	2.6	1.7	1.2	.82	.60	.46
	2	35	34	32	28	17	6.4	2.9	1.6	.94	.62	.43	.32	.24
	1	46	46	46	46	23	0	0	0	0	0	0	0	0

Current = 35 (3a)

TABLE V

Energy Distribution In Current $(dJ/dE)/J_o$

(a) Probe Potential = 0 and Mach 7

Volts	E	$(dJ/dE)/J_o$	$(1/7)(\frac{1}{2}/\sqrt{\pi})\exp\left[-(E^{\frac{1}{2}} - 7.0)^2\right]$
0	0	0	0
2.8	25	.000378	.000378
5.1	45.54	.0378	.0379
5.5	49	.0403	.0403
8.4	75	.00256	.00255

(b) Probe Potential = -5.1 Volts and Mach zero

Volts	E	$(dJ/dE)/J_o$	1.0 or exp (45.54 - E)
0	0	0	1.0
1.12	10	.401	1.0
2.24	20	.991	1.0
3.36	30	.992	1.0
5.1	45.54	.978*	1.0
5.6	50	.0116	.0116
6.16	55	$.779 \times 10^{-4}$	$.779 \times 10^{-4}$
8.4	75	1.61×10^{-13}	1.61×10^{-13}

*Became 1.00 when arc length per step changed from 0.2 to 0.1

(c) Probe Potential = -5.1 Volts and Mach 7

Volts	E	$(dJ/dE)/J_o$
0	0	0
2.8	25	8.0×10^{-17}
5.1	45.54	1.1×10^{-19}
5.5	49	1.8×10^{-8}
8.4	75	.0055

TABLE VI

Ion And Electron Densities For The Laplace Field (Table II)

Probe Potential = -5.1 volts

IONS

		1	2	3	4	5	6	7	8	9	10	11	12	13
(1.5a)	13	1.0	1.1	1.0	.95	.96	1.0	1.1	1.0	1.0	.96	.88	.83	.79
	12	1.1	1.1	1.0	.97	.89	.87	.77	.86	.96	1.0	.91	.85	.77
	11	1.2	1.0	1.0	.96	.94	.88	.86	.96	.95	.92	.89	.85	.78
	10	.65	.68	.66	.63	.82	.76	1.0	1.0	.98	.93	.84	.80	.77
	9	.68	.70	.73	.71	.78	.70	.99	1.1	1.0	.96	.83	.76	.73
	8	.87	.78	.85	1.1	.93	.85	1.1	1.2	1.1	.99	.85	.76	.74
	7	.95	.98	1.3	1.3	1.2	1.1	1.2	1.3	1.2	1.0	.86	.75	.72
	6	1.3	1.1	1.5	1.4	1.3	1.1	1.1	1.0	1.1	1.0	.85	.73	.69
	5	1.3	1.3	1.6	1.2	1.2	1.0	.98	.94	.95	.82	.76	.67	.61
	4	1.5	1.5	1.6	1.2	.97	.85	.95	.92	.84	.82	.75	.66	.60
	3	1.9	1.7	1.8	1.1	.93	.60	.77	.84	.76	.72	.66	.59	.54
	2	2.3	1.9	1.4	.84	.43	.34	.70	.66	.63	.66	.60	.55	.52
	1	2.5	2.5	1.9	1.5	.23	.03	.31	.32	.42	.41	.47	.46	.48

10 min. (3a)

ELECTRONS

		1	2	3	4	5	6	7	8	9	10	11	12	13
(1.5a)	13	0	0	0	0	.01	.03	.06	.09	.13	.16	.19	.23	.25
	12	0	0	0	0	0	.02	.04	.08	.11	.15	.19	.22	.25
	11	0	0	0	0	0	.01	.03	.06	.10	.14	.18	.22	.25
	10	0	0	0	0	0	.01	.02	.05	.06	.13	.18	.21	.25
	9	0	0	0	0	0	0	.02	.04	.08	.12	.16	.20	.25
	8	0	0	0	0	0	0	.01	.03	.06	.11	.16	.21	.24
	7	0	0	0	0	0	0	.01	.02	.05	.10	.15	.20	.25
	6	0	0	0	0	0	0	0	.02	.04	.09	.14	.21	.25
	5	0	0	0	0	0	0	0	.02	.04	.09	.15	.22	.28
	4	0	0	0	0	0	0	0	.01	.05	.09	.15	.22	.28
	3	0	0	0	0	0	0	0	.01	.04	.09	.15	.23	.30
	2	0	0	0	0	0	0	0	.02	.05	.09	.16	.24	.31
	1	0	0	0	0	0	0	0	.02	.05	.11	.17	.25	.32

3.5 min. (3a)

TABLE VII

Poisson Potential For 13 x 13 Grid $r_m = 3a$, $z_m = 1.5a$

Probe Potential = -5.1 volts

(All values are negative for ions, positive for electrons)

		1	2	3	4	5	6	7	8	9	10	11	12	13
(1.5a)	13	5.0	4.8	4.4	3.7	3.0	2.3	1.7	1.3	.95	.75	.63	.56	.45
	12	5.8	5.6	5.0	4.2	3.3	2.4	1.7	1.1	.75	.54	.44	.41	.43
	11	6.9	6.6	6.0	5.0	3.8	2.7	1.7	1.1	.63	.39	.30	.31	.40
	10	8.3	8.0	7.2	6.0	4.5	3.1	1.9	1.1	.56	.29	.20	.23	.36
	9	10	9.8	8.8	7.3	5.4	3.5	2.1	1.1	.53	.22	.13	.18	.32
	8	12	12	11	8.9	6.4	4.1	2.3	1.2	.52	.19	.09	.13	.28
	7	15	15	13	11	7.7	4.7	2.6	1.3	.54	.19	.07	.10	.24
	6	19	18	16	13	9.2	5.3	2.7	1.3	.56	.21	.07	.09	.21
	5	23	22	20	17	11	5.8	2.8	1.3	.56	.23	.09	.08	.17
	4	28	27	25	21	13	6.1	2.7	1.2	.52	.23	.10	.07	.13
	3	33	33	31	26	16	5.7	2.2	.90	.41	.20	.09	.06	.09
	2	39	39	38	34	19	4.1	1.3	.50	.23	.12	.06	.03	.04
	1	46	46	46	46	23	0	0	0	0	0	0	0	0

Current = 24 (3a)

TABLE VIII

Ion And Electron Densities For The Poisson Field (Table VII)

Probe Potential = -5.1 volts

IONS

		1	2	3	4	5	6	7	8	9	10	11	12	13
(1.5a)	13	.88	.90	.87	.90	1.0	1.0	1.1	1.1	1.1	1.1	.98	.90	.73
	12	.92	.91	.87	.81	.76	.81	.89	.93	.95	.90	.83	.79	.71
	11	.75	.65	.70	.69	.57	.77	.86	.84	.87	.82	.75	.72	.71
	10	.57	.59	.59	.58	.70	.60	.81	.83	.80	.81	.75	.70	.71
	9	.61	.60	.67	.48	.54	.55	.73	.82	.80	.79	.74	.69	.71
	8	.67	.58	.57	.57	.46	.53	.67	.76	.79	.78	.74	.68	.70
	7	.73	.64	.67	.63	.50	.55	.61	.68	.75	.73	.71	.67	.67
	6	.69	.57	.63	.67	.60	.46	.53	.52	.61	.65	.64	.63	.63
	5	.54	.57	.61	.50	.51	.43	.41	.42	.46	.48	.52	.56	.60
	4	.57	.55	.45	.54	.41	.26	.32	.34	.33	.35	.41	.50	.54
	3	.59	.55	.46	.53	.28	.25	.27	.29	.28	.30	.36	.44	.53
	2	.88	.77	.40	.39	.04	.12	.29	.26	.26	.28	.32	.41	.48
	1	1.3	1.5	1.2	.75	.05	.03	.19	.23	.24	.25	.30	.38	.45

(3a)

ELECTRONS

		1	2	3	4	5	6	7	8	9	10	11	12	13
(1.5a)	13	.01	.01	.01	.03	.05	.08	.10	.12	.15	.16	.20	.22	.32
	12	0	0	.01	.02	.04	.08	.12	.16	.18	.19	.23	.27	.30
	11	0	0	0	.01	.02	.06	.12	.17	.19	.23	.26	.28	.30
	10	0	0	0	0	.01	.05	.11	.17	.20	.23	.26	.27	.29
	9	0	0	0	0	0	.03	.09	.16	.19	.21	.24	.28	.28
	8	0	0	0	0	0	.02	.07	.15	.19	.19	.22	.27	.28
	7	0	0	0	0	0	.01	.06	.13	.18	.21	.24	.27	.28
	6	0	0	0	0	0	0	.04	.11	.21	.27	.28	.31	.29
	5	0	0	0	0	0	0	.03	.10	.21	.38	.28	.30	.30
	4	0	0	0	0	0	0	.02	.10	.22	.35	.33	.32	.32
	3	0	0	0	0	0	0	.01	.12	.29	.39	.35	.34	.32
	2	0	0	0	0	0	0	.02	.19	.40	.47	.40	.35	.34
	1	0	0	0	0	0	0	.04	.21	.32	.33	.35	.34	.36

(3a)

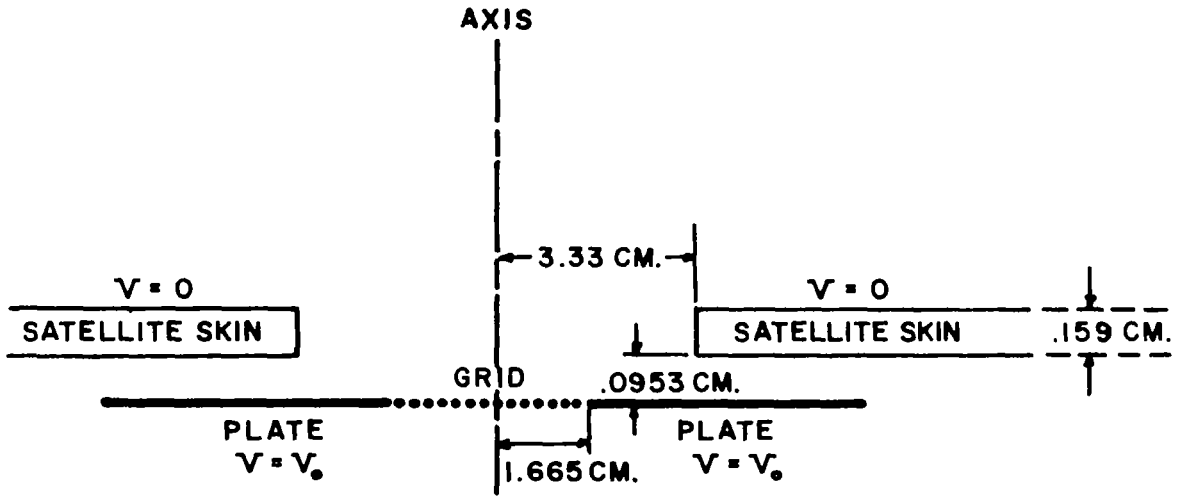

FIGURE 1. OGO PLANAR PROBE GEOMETRY

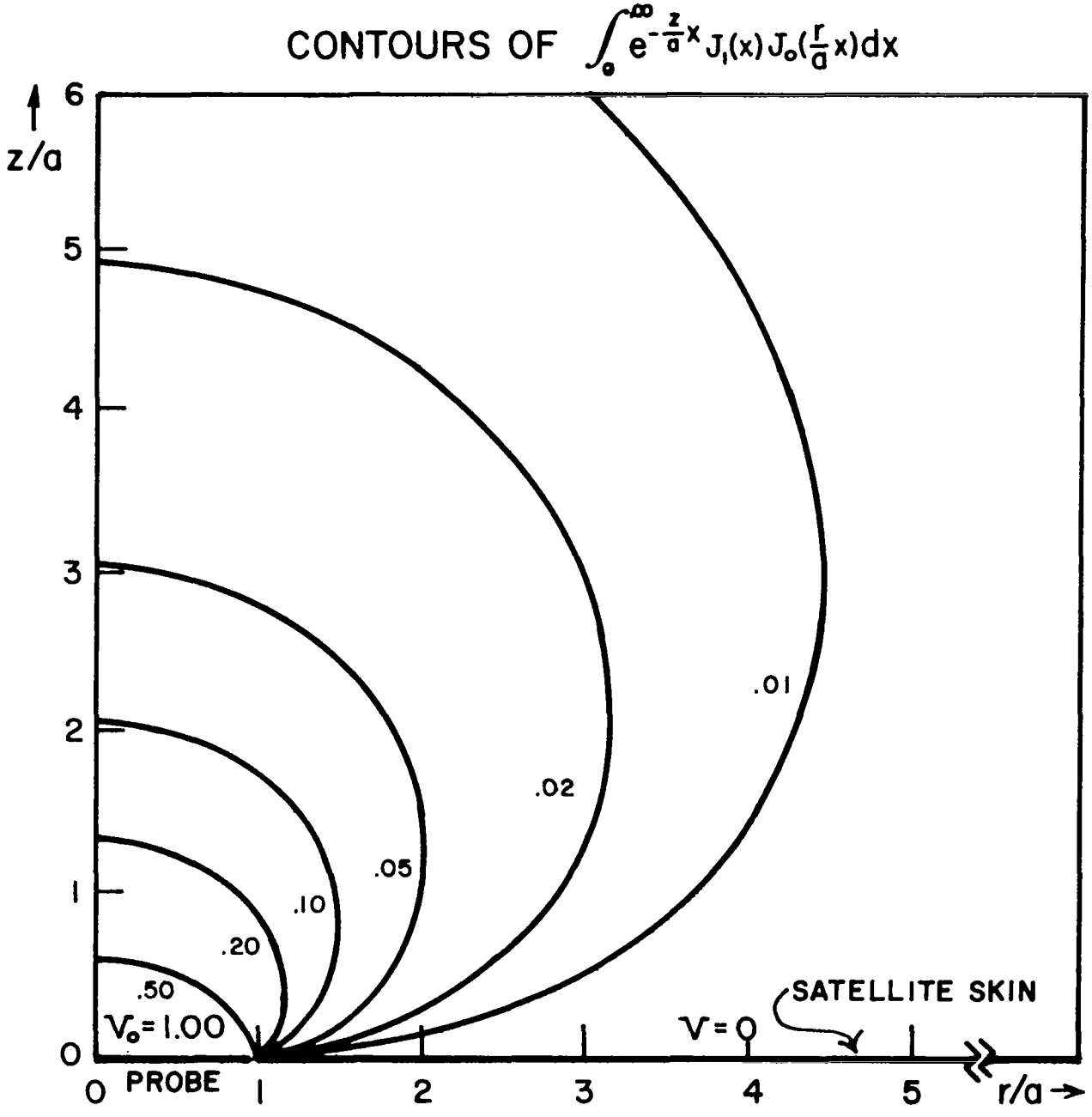

FIGURE 2. LAPLACE POTENTIAL

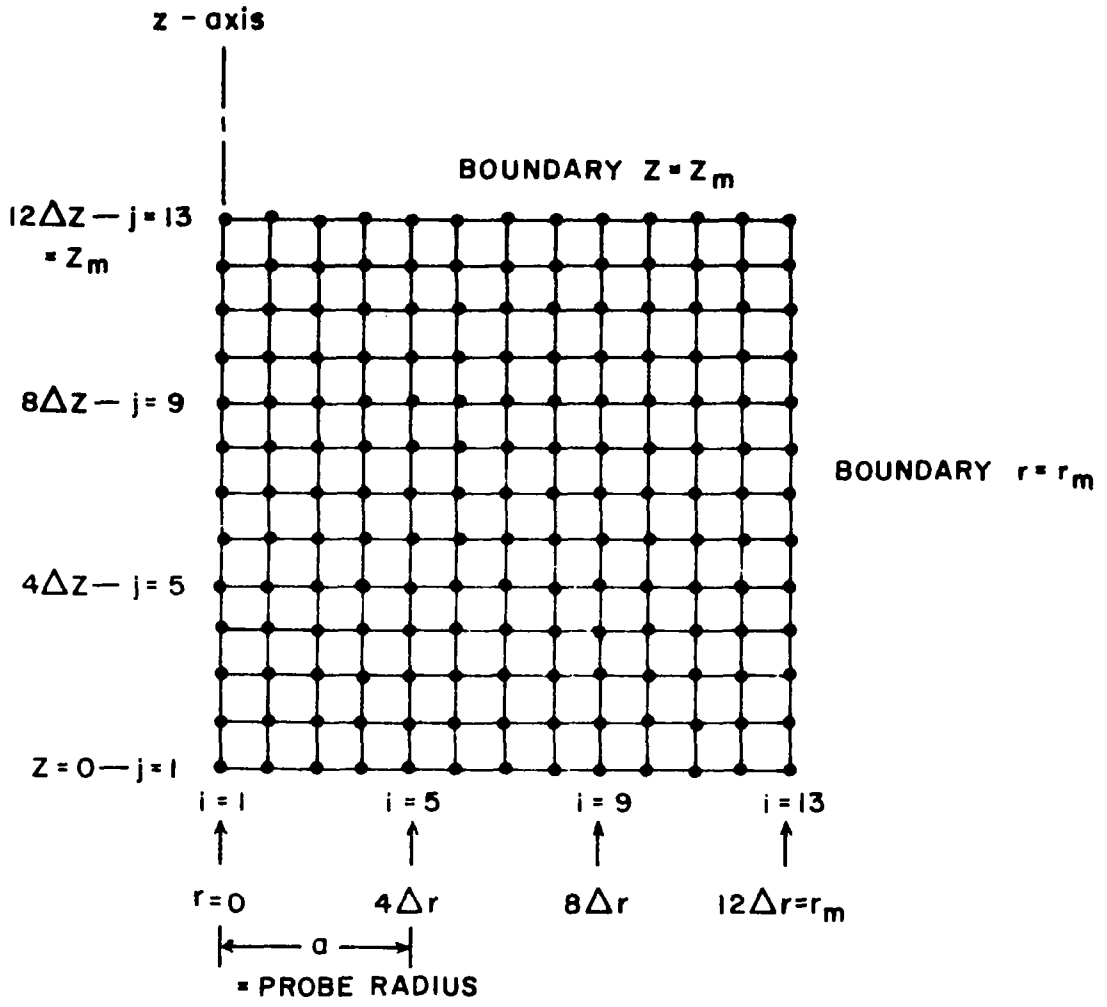

First row j = 1: (probe potential = -5.1 volts)

$\Phi_1 = \Phi_2 = \Phi_3 = \Phi_4$ = -45.54 for ions, +45.54 for electrons

Φ_5 = -22.77 for ions, +22.77 for electrons

$\Phi_6 = \Phi_7 = \ldots = \Phi_{13} = 0$

FIGURE 3. 13 x 13 GRID

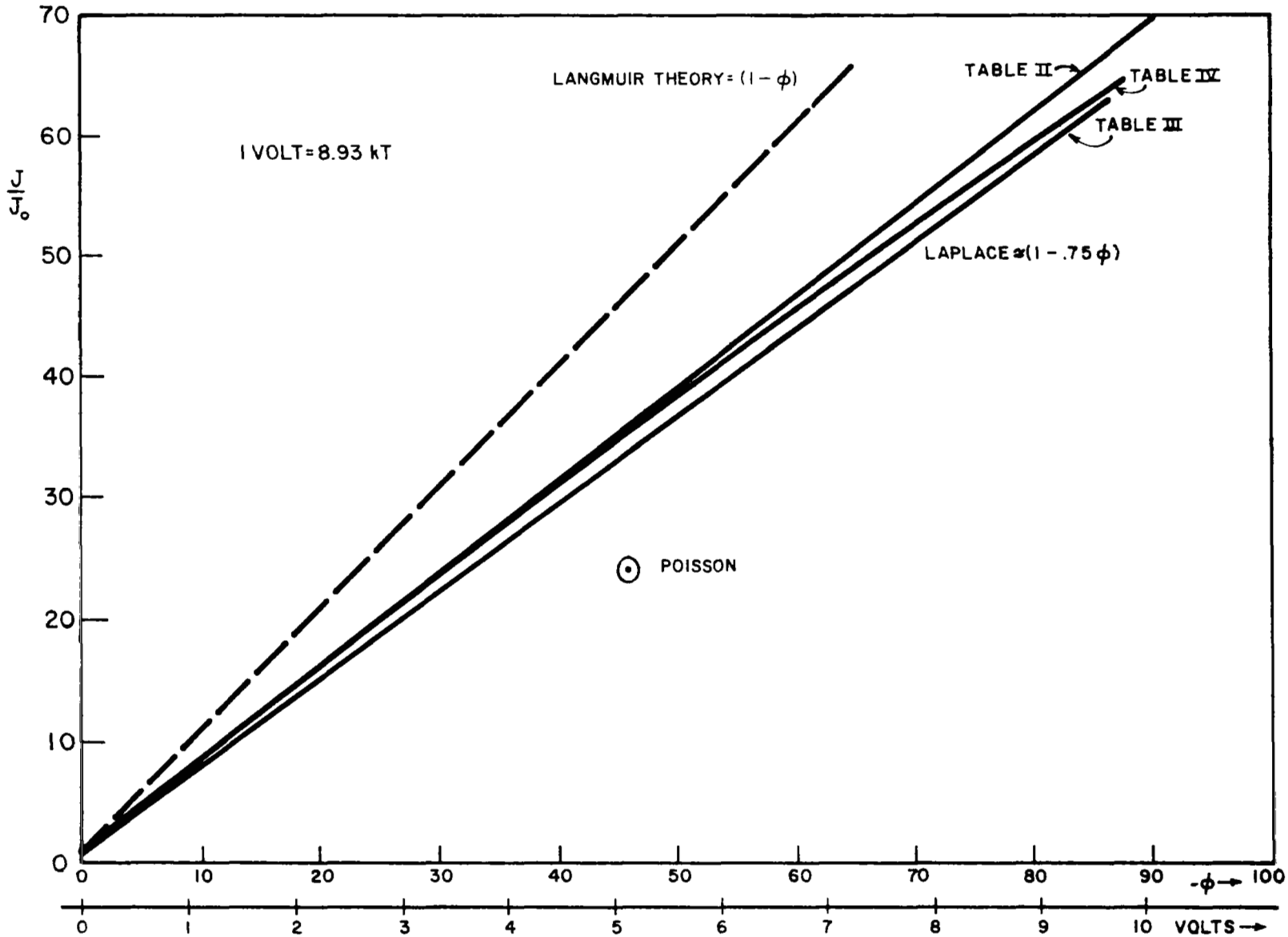

FIGURE 4. CURRENT-VOLTAGE CHARACTERISTICS (ZERO MACH NUMBER)

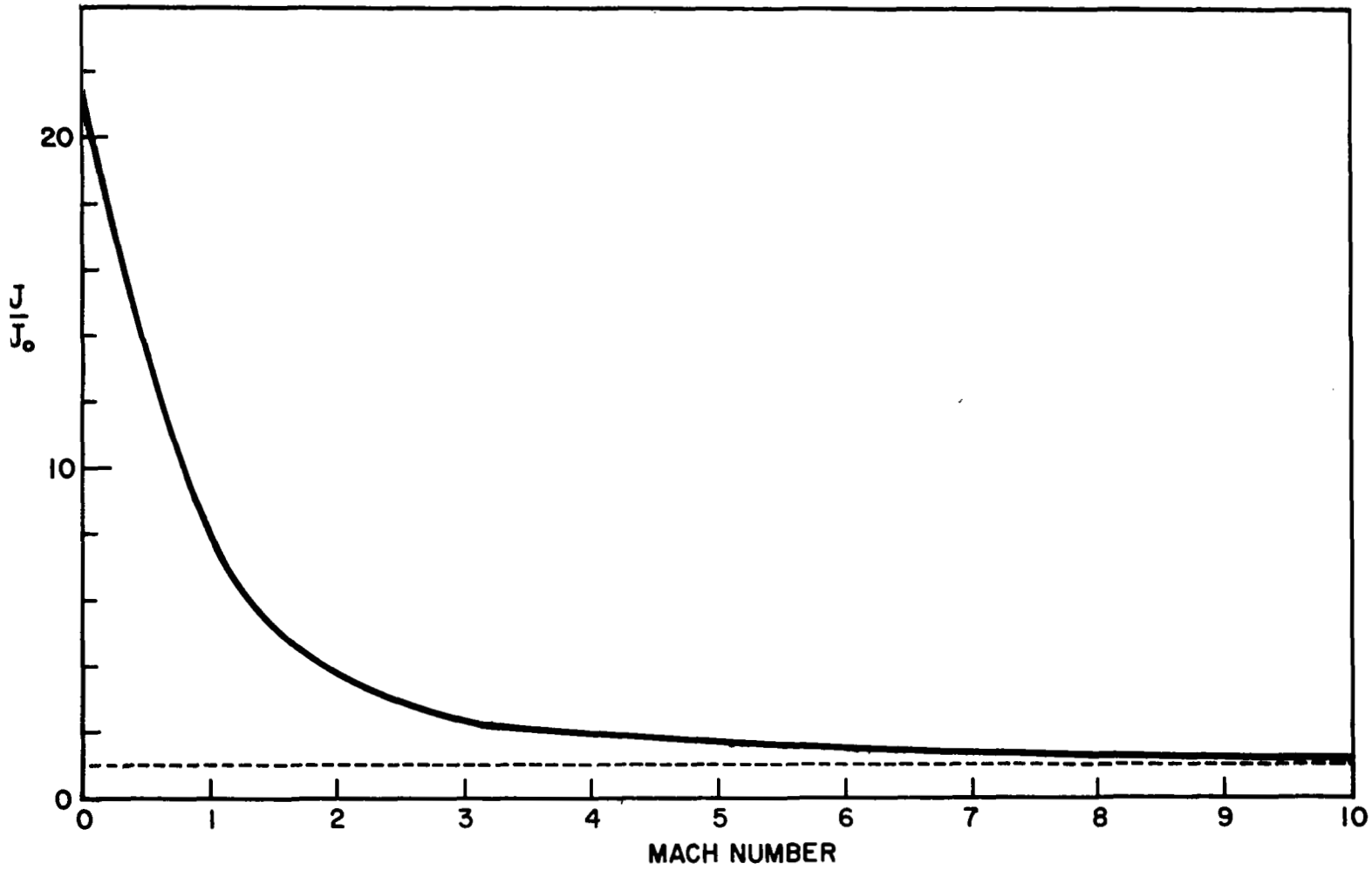

FIGURE 5. CURRENT vs MACH NUMBER POTENTIAL = -5.1 VOLTS

REFERENCES

1. Al'pert, Ya. L., A. V. Gurevich, and L. P. Pitaevskii, Space Physics With Artificial Satellites, Consultants Bureau, New York, 1965

2. Shea, J., "Missile-Plasma Interaction Phenomena", Cosmic, Inc. Report No. 79, November 1964

3. Davis, A. H., and I. Harris, Rarefied Gas Dynamics, Ed. L. Talbot, Academic Press, New York, 1961

4. Rand S., Phys. Fluids 2, 649 (1959); Phys. Fluids 3, 265 (1960)

5. Mott-Smith, H. and I. Langmuir, Phys. Rev. 28, 727 (1926)

6. Bernstein, I. B. and I. N. Rabinowitz, Phys. Fluids 2, 112 (1959)

7. Hall, L. S., "Probes and Magnetic Pumping in Plasma", Univ. of California Radiation Lab. Report, UCRL 6535, July 1961

8. Laframboise, J., "Theory of Electrostatic Probes in Collisionless Plasmas at Rest", Fourth International Symposium on Rarefied Gas Dynamics, Toronto, July 1964, To be published

9. See, for example, Forsythe, G. and W. Wasow, Finite Difference Methods for Partial Differential Equations, Wiley, 1960

10. Designed by E. C. Whipple, Jr., at the Goddard Space Flight Center

11. See, for example, Ralston, A. and H. S. Wilf, editors, Mathematical Methods for Digital Computers, Part III, Wiley, 1964